Doppler effect on Matched Field Processing in Ocean Acoustics

Hee Chun Song*

Abstract

Matched field localization schemes often show a high sensitivity to acoustic variabilities due to mismatch between assumed and actual environments. In this paper, we focus on the effect of source motion or Doppler on matched field processing (MFP). To accomplish this, MFP is extended to treat a moving source problem with normal mode description of the sound field. The extension involves both the temporally nonstationary and spatially inhomogeneous nature of the sound field generated by a time-harmonic point source moving uniformly in a stratified oceanic waveguide. It is demonstrated that the impact of source motion can be significant to MFP although the velocity of a moving source is much smaller than the sound velocity of the oceanic waveguide. In addition, a criteria for minimizing the effect of Doppler on MFP is discussed.

Ⅰ. Introduction

Matched field processing (MFP) is an approach for detemining the location of an acoustic source. This topic has been an active area of research for more than a decade. MFP methods are based on comparing acoustic data from an array of hydrophones with solutions of wave equation that correspond to test source locations. The unknown parameters of MFP usually consist of coordinates of the source. As discussed in several recent articles [1, 2, 3, 4, 5, 6], major difficulties facing this approach are that the localization process is sensitive to errors in the propagation model such as sound speed, water depth, and geoacoustic bottom parameters. In this paper we focus on the effect of source motion or Doppler on MFP, which has been considered negligible because the velocity of a moving source is much smaller than the sound speed of the waveguide.

This paper is concerned with the development of the analytic approach to the moving source problem with a model constraining the dynamics, the geometry, and the noises. The source radiates a continuous wave (cw) signal with a known frequency, and the source motion is assumed to be steady (unaccelerated). The observations are made at a stationary vertical array in a background of spatially incoherent Gaussian noise. It employs the normal model descriptions of the sound field in the forward modeling of the fields due to a moving source, and develops an optimum processor based on the maximum likelihood estimation techniques to estimate a set of source parameters such as range, depth, and velocity.

The paper is organized as follows. The acoustic field due to a moving source is presented in Section II. After formulation of the problem in Section III, the effect of source motion is investigated in Section IV using generalized ambiguity function. Simulation results for an Arctic environment is presented in Section V, followed by conclusions.

Ⅱ. Acoustic Field due to a Moving Source

Figure 1 depicts a source and a receiver in a stratified ocean. The ocean is modeled as a waveguide, and the signal from the source can be considered to be the point source solution to the wave equation. The medium is assumed to be horizontally stratified and time independent. Let p be the pressure for a time harmonic, moving point source, which satisfies the inhomogeneous wave equation: we then have a unit normalized source strenght

$$\left[\nabla^2 - c^{-2}(z)\frac{\partial^2}{\partial t^2}\right] p(\mathbf{r}, t) = -4\pi\delta[\mathbf{r}-\mathbf{r}_s(t)]\, exp(-i\omega_0 t) \quad (1)$$

*Korea Ocean Research & Development Institute
Manuscript Received: October 20, 1995.

The source is located at $\mathbf{r}_s(t)$ and has an intrinsic frequency $\omega_0 = 2\pi f_0$. With horizontal stratification, the wave equation can be separated into range and depth. The wave equation above has been solved formally in terms of normal modes by Hawker [7].

$$p(r, z, t) = Q\left(\frac{2\pi}{|r - r_0|}\right)^{1/2} exp\left[-i\left(\omega_0 t + \frac{\pi}{4}\right)\right] \sum_n \Gamma_n \tag{2}$$

where

$$\Gamma_n = \frac{\phi_n(z)\phi_n(z_0)}{\sqrt{k_n}}\, e^{-\delta_n |r - r_0|} e^{ik_n |r - r_0| f(\theta)} \tag{3}$$

$$f(\theta) = 1 - \eta_n \sin\theta + \frac{1}{2}\,\eta_n^2[1 - (1 - D_n)\sin^2\theta] + \cdots \tag{4}$$

$$\eta_n = -\frac{v}{v_n^G} \tag{5}$$

$$D_n = k_n \frac{\partial v_n^G}{\partial \omega} \tag{6}$$

In the equations above, the source, moving with the velocity v, has coordinates (r_0, z_0) at $t = 0$ and the receiver is set at (r, z). The quantities found in the equations are the usual ones found in standard mode theory with the addition of $f(\theta)$ in the phase to describe the source motion. Specifically, ϕ_n is the n^{th} mode function, k_n is the horizontal wavenumber associated with the n^{th} mode, δ_n is the attenuation parameter of the n^{th} mode, v_n^G is the group velocity of the n^{th} mode, and θ is a source-receiver geometry angle defined in Figure 1. Q is a constant associated with source strength.

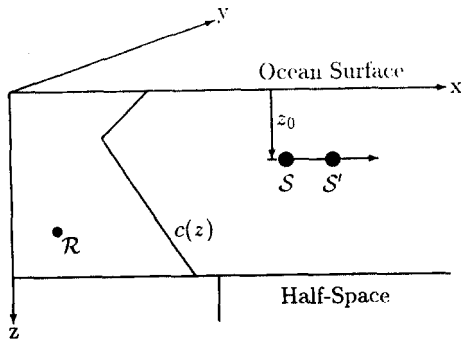

(a) Side View

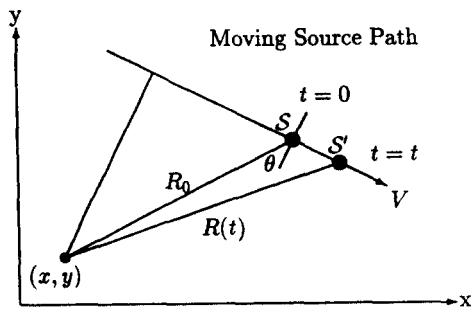

(b) Top View

Fig. 1. Source and receiver geometry and ocean environment model: (a) side view, (b) top view.

Ⅲ. Formulation of the Problem

3.1 The Analytic Model

In the previous section, the pressure fineld generated by a moving source has been presented in terms of normal modes. The source is assumed to continuously emit a narrow-band signal of a known frequency. The vertical array of dimension L spans the waveguide from the top, i.e., from $z = 0$ to $z = L$, and is located at (x, y) on the projected surface plane (Fig. 1(b)). Using complex (analytic) signal representation, the received signal demodulated at the source frequency $f_0 = \omega/2\pi$ can thus be written as

$$\tilde{r}(t, z) = \sqrt{E_r}\,\tilde{b}\,\tilde{s}_n(t, z, \mathbf{A}) + \tilde{w}(t, z),$$

$$t \in \left[-\frac{T}{2}, \frac{T}{2}\right],\ z \in [0, L] \tag{7}$$

where we assume that 1) $\tilde{b}$ is a zero mean complex Gaussian random variable independent of measurement noise $\tilde{w}(t, z)$, 2) $\tilde{w}(t, z)$ is a zero mean, spatially and temporally white Gaussian noise process with double spectral height of N_0, and 3) $\mathbf{A} = [R_0, Z_0, V \sin\theta]^T$ is the parameter vector defining the geometry of the source and the receiver (it is unknown and nonrandom). Multiplicative random-type disturbance $\tilde{b}$, with variance $E[|\tilde{b}|^2] = 2\sigma_b^2$, accounts for model inaccuracies, e.g., radiated signal power variations about some nominal value, fading the transmission medium, etc. More inportantly, the presence of $\tilde{b}$ represents the lack of knowledge of the signal absolute phase.

$\tilde{s}_n(t, z, \mathbf{A})$ is a complex envelope of the received signal normalized in both time and space as

$$\int_{-T/2}^{T/2} dt \int_0^L dz\, \tilde{s}_n(t, z, \mathbf{A})\, \tilde{s}_n^*(t, z, \mathbf{A}) = 1. \tag{8}$$

and E_r is the total energy received during the observation interval T, by a vertical array of dimension L.

3.2 Optimum receiver

We apply the maximum likelihood (ML) technique to estimate the parameter vector A, where we choose as our estimate $\hat{\mathbf{A}}$ the value of A that most likely caused a given observation to occur. The first step is to find a likelihood function. Since there is one-to-one correspondence between the likelihood function and the likelihood ratio [8], we obtain the likelihood function as

$$\ln \Lambda_l(\hat{\mathbf{A}}) = \frac{1}{N_0} \frac{\bar{E}_r}{N_0 + \bar{E}_r} |\tilde{L}(\hat{\mathbf{A}})|^2 \tag{9}$$

where

$$\tilde{L}(\hat{\mathbf{A}}) = \int_{-T/2}^{T/2} dt \int_0^L dz\, \tilde{r}(t, z)\, \tilde{s}_n^*(t, z, \hat{\mathbf{A}}) \tag{10}$$

and

$$\bar{E}_r(T) = \text{average received energy} = 2\sigma_p^2 E_r(T) \tag{11}$$

The coefficient in Eq.9 is of importance only when we compute the Cramér-Rao bound, which is studied extensively in [9]. Therefore we can suppess it for our discussion. The values of $\hat{\mathbf{A}}$ where the above likelihood function has its maximum are $\hat{\mathbf{A}}_{ml}$.

To find $\mathbf{A}_{ml}$ we must generate $\ln \Lambda_l(\hat{\mathbf{A}})$ for the values of $\hat{\mathbf{A}}$ in the region of interest, Ω space. For any particular $\hat{\mathbf{A}}$, say $\hat{\mathbf{A}}_j$, we can generate $\ln \Lambda_l(\hat{\mathbf{A}})$ through a complex receiver using a correlation operation shown in Fig. 2. We define a function called a generalized correlation function denoted by $\Psi(\mathbf{A})$,

$$\Psi(\mathbf{A}, \hat{\mathbf{A}}) \equiv \langle \tilde{s}_n(\mathbf{A}), \tilde{s}_n(\hat{\mathbf{A}}) \rangle \tag{12}$$

which is a measure of the degree of similarity between a complex envelope with parameter vector A and its replica $\hat{\mathbf{A}}$. Then the output of the ML receiver is the squared modulus of the generalized correlation function

$$\Phi(\mathbf{A}, \hat{\mathbf{A}}) = |\Psi(\mathbf{A}, \hat{\mathbf{A}})|^2 \tag{13}$$

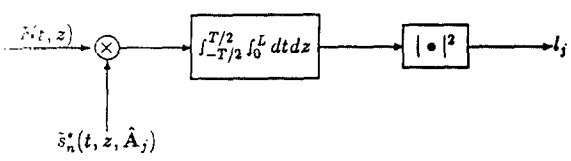

Fig. 2. Correlation receiver (complex operation)

In analogy with radar and active sonar theory, the function $\Phi(\mathbf{A}, \hat{\mathbf{A}})$ is referred to as a generalized ambiguity function [10, 11] which illustrates the global properties of a maximum likelihood estimator. We can analyze problems of accuracy, ambiguity, and resolution using the generalized ambiguity function.

Ⅳ. Generalized Ambiguity Function (GAF)

In this section we study the ambiguity structure to investigate the effect of source motion on matched field processing For simplicity, consider the case of a source moving radially away with respect to a stationary vertical array, i.e., $\theta = \pi/2$ and $R = R_0 + Vt$. If the source is not moving radially, the radial component of the speed ($V \sin\theta$) can be estimated. Considering that the source speed is much smaller than the group speed in ocean environment, we assume $f(\theta) = 1$, i.e., $k_n' = k_n$. Using the orthogonality conditions of modal functions with the assumption that the vertical array is sufficiently long and densely populated, GAF is greatly simplified to

$$\Psi(\mathbf{A}, \hat{\mathbf{A}}) = G(\mathbf{A})G(\hat{\mathbf{A}}) \sum_{p=1}^{D} \frac{\phi_p(Z_0)\phi_p(\hat{Z}_0)}{k_p} e^{-\delta_p(R_0 + \hat{R}_0)} e^{jk_p\Delta R_0} sinc[k_p(\Delta V)T/2] \tag{14}$$

and

$$G(\mathbf{A}) = G(Z_0) = \left(\sum_{p=1}^{D} \frac{\phi_p^2(Z_0)}{k_p} e^{-2\delta_p R_0} \right)^{-1/2} \tag{15}$$

where

$$\Delta R_0 = R_0 - \hat{R}_0 \tag{16}$$

$$\Delta V = V - \hat{V}. \tag{17}$$

We notice immediately that if there is no mismatch of source motion, i.e., $\Delta V = 0$, the GAF resembles either the indicator function in matched mode localization [2] or the range-depth function defined in modal beamforming [13]. In that case GAF defines a two dimensional surface as a function of range and depth, which is obtained by applying conventional beamforming (Bartlett) with perfect mode filtering conditions. The matched mode localization is equivalent to the conventional matched field processing under this condition, which also has been demonstrated by Smith et. al. [14] and Yang [15]. The peak of this surface yields source range

and depth simultaneously.

Now we study the effect of mismatch of source speed on range/depth ambiguity structure since we are primarily concerned with effects of source motion or Doppler on matched field processing for range/depth localization. The effect of source motion is contained in the argument of *sinc* function with discrete horizontal wavenumber k_n and time window T. We define X as an uncompensated Doppler distance, i.e., $X=\Delta V \times T$. Then the effects of mode coupling through source motion would depend on the spreading of the eigenvalues k_p in conjunction with Doppler distance X. The discrete eigenvalues k_p lie between ω/C_B and ω/C_{min}, where C_B denotes the sound velocity at the bottom half-space and C_{min} represents the minimum sound velocity within the water column. When the argument of the "sinc" function has negligible variation among the modes, this term acts as a scale factor and does not significantly affect the behavior of the range/depth ambiguity.

However, the reduction of GAF results in a decrease of signal-to-noise ratio and would degrades the performance of the receiver. On the other hand, if the argument has strong dependence on modes, the mismatch of source motion would significantly affects the ambiguity structure in range/depth plane. These aspects are investigated through simulations in the following section. We should be careful that the time window T itself contributes to the scale factor through the average signal energy $\bar{E}_r$, defined in Eq. 11 which is linearly proportional to T, *i.e.*,

$$\bar{E}_r(T)=\left[\frac{2\sigma_b^2 Q^2}{G^2(Z_0)R_0}\right]T \tag{18}$$

V. Simulations

We pick a horizontally stratified Arctic ocean environment shown in Fig.3 with an arbitrary velocity profile that includes convergence zone modes of propagation, which has been introduced for matched field processing in [16] due to significant variability of the sound field. For simulation, we choose 50 Hz as the source frequency and put the source at 30 km away from a stationary receiver. The waveguide supports a total of 19 modes. The source is assumed to move with a constant radial speed of 5 kts (2.57 m/s). In fact, the important parameter here is not the absolute speed V, but the mismatched speed ΔV multiplied by the observation time window T.

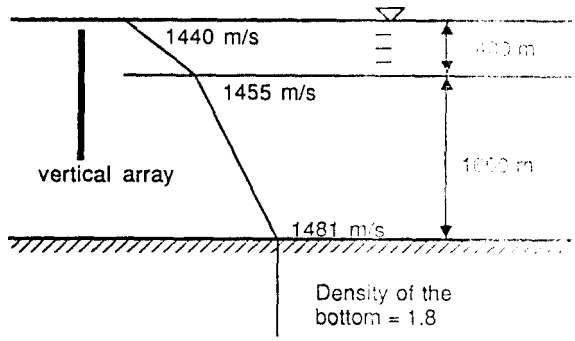

Fig. 3. Arctic ocean environment for simulations

First we consider the case when the source is stationary (fixed) or the velocity is assumed known a priori. The parameter vector is now $\mathbf{A}=[R_0, Z_0]$. Then the generalized correlation function defined in Eq.12 reduces to

$$\Psi(\mathbf{A}, \hat{\mathbf{A}})=G(\mathbf{A})G(\hat{\mathbf{A}})\sum_{p=1}^{D}\frac{\phi_p(Z_0)\phi_p(\hat{Z}_0)}{k_p}e^{jk_p\Delta R_0} \tag{19}$$

wher modal attenuations are assumed to be negligible among the modes. Fig. 4(a) and 4(b) show contour plot of the equal ambiguity surface in range/depth plane for different source depths at the same range of 30 km with contour interval of 2 dB. Throughout the simulations, 50 dB corresponds to the peak level at the true source location. The range and the depth are sampled by 1 km and 20m, respectively. Note that the minimum range of the ambiguity surface is set to 10 km to include the contributions of discrete modes only. The ambiguity function is symmetric about the true range(i.e., $\Delta R=0$). When the source is at 100-m depth (Fig. 4(a)), the ambiguity surface is characterized by a significant number of ambiguous maxima (within 3 dB from the true peak) in range which apparently exhibit some periodicity associated with modal cycle distances. Compared to this result, in Fig. 4(b) we have one strong peak at the true source location, with another strong peak around 60 km range, so-called convergence zone (3 dB down).

Now we proceed to the case when the source is moving and the velocity is not known a priori. Fig. 5(a) show the range/depth ambiguity surface for a source at 30km range and 100m depth with a mismatch of Doppler distance $X=30m$. The ambi-

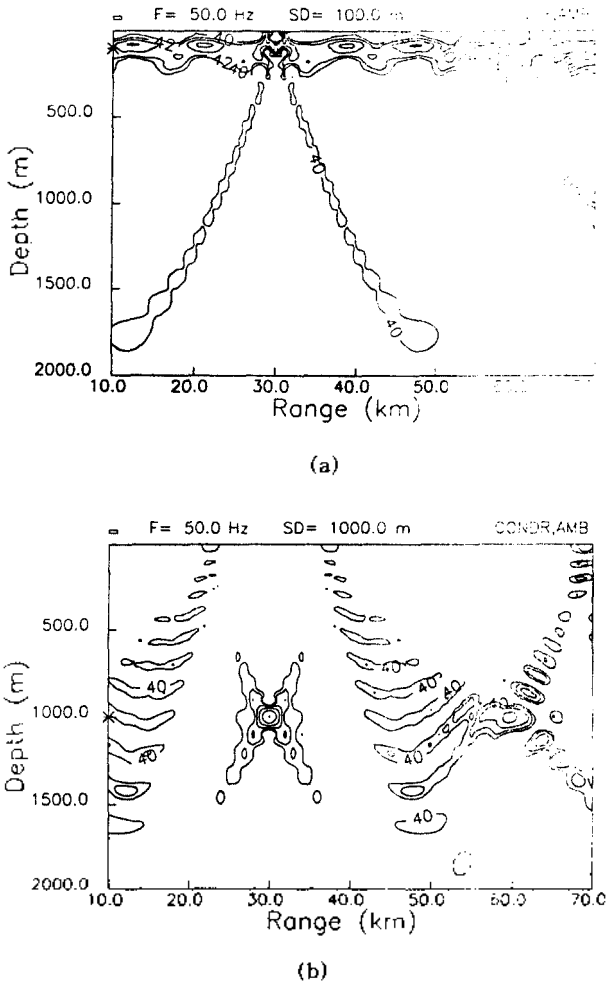

Fig. 4. Range/Depth ambiguity surface for a source at the range of 30km and the depth of (a) 100m and (b) 1000m, respectively, with the source either stationary or source velocity known a priori. The peak level at the true location is 50 dB.

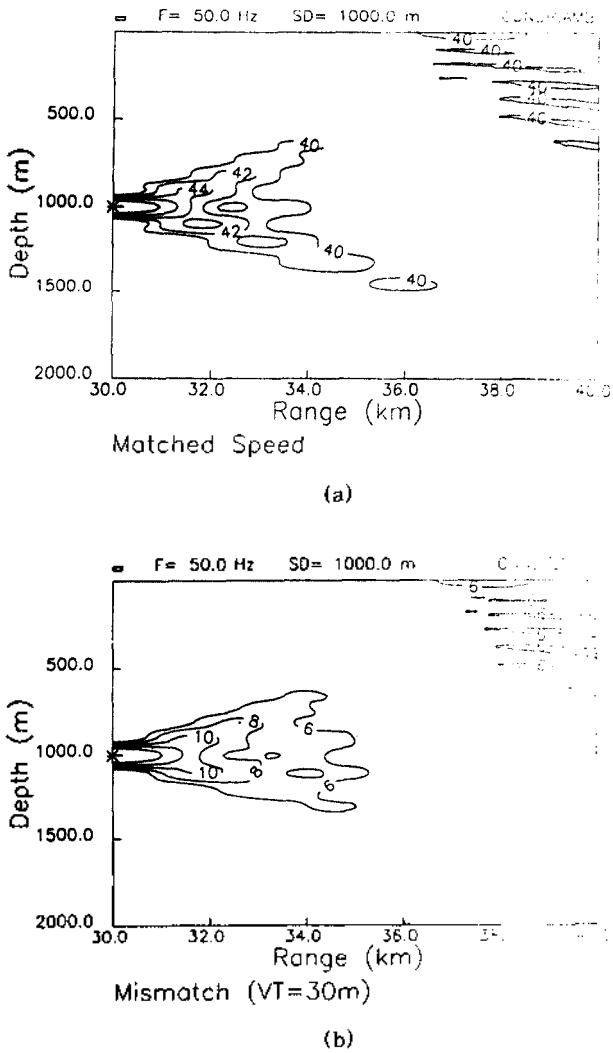

Fig. 5. Range/Depth ambiguity surface for a source depth of 1000m (a) with a Doppler distance mismatch of $\Delta V \times T = 30$m and (b) without mismatch.

guity surface is sampled with interval of 200m and 20m in range and depth, respectively. Note that the ture target is located at the origin and the ambiguity surface is one-sided in range due to the symmetry property. Compared to the case without mismatch shown in Fig. 5(b), there is no significant change in the range/depth ambiguity structure except the change in peak contour level, which is about 30dB. Recalling the the ambiguity function defined in Eq. 13 considere the signal part only, this reduction means lowering signal to noise ratio, and thus can degrade the performance quite drastically. The reason is as foolows. The effects of source speed is confined in terms of "sinc" function where the argument is $k_p X/2$. The first null of this sinc function corresponds to the horizontal wavelength: $2\pi/k_p \simeq 30m$, which explains the great reduction at $X = 30m$. Secondly, there is a slight difference between the lowest (mode 19) and the highest (mode 1) eigenvalues. Then we can take the sinc function term out of summation due to the negligible dependence on mode number, making this term act just like a scale factor. In other words, Doppler spreading of the modes is narrow enough to be considered as a single Doppler shift. This explains why there is no essential change in the ambiguity structure, but the magnitude has decreased. From these results we can draw an important conclusion that the performance of a source range/depth localization remains almost the same as long as the mismatch of Doppler distance (uncompensated source speed × time window) is less than the half-wavelength of trapped modes. In

other words, we can treat a moving source problem as a stationary problem in this case.

VI. Conclusions

In this paper, the effect of Doppler or source motion is investigated. With the models constraining the geometry, the dynamics, and the signals, we formulated the moving source localization problem in the context of multiparameter estimation problem. The optimum receiver based on the maximum likelihood estimates produces GAF which illustrates the global properties of the estimator. The principal result is that uncompensated source motion could significantly degrade the performance of MFP. In addition, a moving source problem can be treated as a stationary source problem if the uncompensated Doppler distance X is less than half the wavelength of the discrete trapped modes.

References

1. Donald R. Del Balzo, Christopher Feuillade, and Mary M. Rowe. Effects of water-depth mismatch on matched-field calization in shallow water. *Journal of Acoustical society of America*, 83(6):2180-2185, 1988.
2. A. Tolstoy. Sensitivity of matched field processing to sound-speed profild mismatch for vertical arrays in a deep water Pacific environment. *Journal of Acoustical Societty of America*, 85(6):2394-2404, June 1989.
3. Patrick M. Verlardo Jr. Robust matched field source localization. Master's thesis, MIT, 1989.
4. Donald F. Gingas. Methods for predicting the sensitivity of matched-field processors to mismatch. *Journal of Acoustical Society of America*, 86(5):1940-1949, November 1989.
5. John R. Daugherty and James F. Lynch. Surface wave, internal wave, and source motion effects on matched field processing in a shallow water waveguide. *Journal of Acoustical Societty of America*, 87(6):2503-2526, June 1990.
6. C. Feuillade, D. R. Del Balzo, and Mary M. Rowe. Environmental mismatch in shallow-water matched-field processing:Geoacoustic parameter variability. *Journal of Acousttical Society of America*, 85(6): 2454-2364, June 1989.
7. Kenneth E. Hawker. A normal mode theory of acoustic Doppler effects in the oceanic waveguide. *Journal of Acousttical Societty of America*, 65(3):675-681, 1979.
8. H. L. Van Trees. *Detection, Estimation and Modulation Theory, Part I*. John Wiley and Sons, New York, 1970.
9. Hee chun Song. Performance bounds for passively locating a moving source of a known frequency in oceanic waveguide using a vertical array. *IEEE J. of Oceanic Eng.*, 18(3):189-198, July 1993.
10. P. M. Woodward. *Probability and Information Theory with Applications to Radar*. Pergamon, Oxford, England, 1964.
11. H. L. Van Trees. *Detection, Estimation and Modulation Theory, Part III*. John Wiley and Sons, New York, 1971.
12. Gary R. Wilson, Rober A. Koch, and Paul J. Vidmar. Matched mode localization. *Journal of Acoustical Society of America*, 84(1):310-320, July 1988.
13. T. C. Yang. A method of range and depth estimation by modal decomposition. *Journal of Acoustical Society of America*, 82(5):1736-1745, 1987.
14. G. B. Smith, C. Feuillade, D. R. DelBalzo, and C. L. Byrne. A nonlinear matched-field processor for detection and localization of a quiet source in a noisy shallow-water environment *Journal of Acoustical Society of America*, 85(3):1158-1166, March 1989.
15. T. C. Yang. Effectiveness of mode filtering:A comparison of matched-field and matched-mode processing. *Journal of Acoustical Society of America*, 87(5): 2072-2084, May 1990.
16. A. B. Baggeroer, W. A. Kuperman, and Henrik Schmidt. Matched field processing:Source localization in correlated noise as an optimum estimation problem *Journal of Acoustical Society of America*, 82(2):571-587, 1988.

▲Hee Chun Song

Hee Chun Song received the B.S. and M.S. degrees in naval architecture and marine engineering in 1978 and 1980, respectively, from Seoul National University, Seoul, Korea, and the Ph.D. degree in ocean engineering in 1990 from the Massachusetts Institue of Technology, Cambridge, USA. Presently he is a senior research scientist in Physical Oceanography Division at Korea Ocean Research and Development Institute (KORDI), Seoul, Korea. His research interests are in applications of signal processing in underwater acoustics and in applying HF Doppler Radar system to measure dynamic properties of the ocean surface.